 CMES, vol.3, no.1, pp.87-99, 2002

A dimensional reduction of the Stokes problem

Olivier Ricou [1] **Michel Bercovier** [2]

Abstract: In this article, we present a method of reduction of the dimension of the Stokes equations by one in a quasi-cylindrical domain. It takes the special shape of the domain into account by the use of a projection onto a space of polynomials defined over the thickness. The polynomials are defined to fit as well as possible with the variables they approximate. Hence, this method restricted to the first polynomial, recovers the Hele-Shaw approximation.

The convergence of the approximate solution to the continuous one is shown. Under a regularity hypothesis, we also obtain error estimates.

A description of the stiffness matrix is exhibited and some computations show the acceleration due to this method. Finally a few numerical results are given.

keyword: dimentionnal reduction, Stokes, Hele-Shaw

1 Introduction

In general, the simulation of 3D flow problems—in particular those including free surfaces—is a computationally intensive task due to the large number of unknowns in the associated linear systems. For certain families of flow problems, this number of unknowns can be drastically reduced. In this article, we consider Stokes flows in quasi-cylindrical domains, i.e., flows between two surfaces. When the thickness is small enough and the two surfaces are planes, this set of flow has been studied for long and are known as the Hele-Shaw flows. Such flows are having by hypothesis a given parabolic profile in the thickness direction. They are approximated by estimating the order of magnitude of each term in the governing equations and reducing the problem to a Poisson equation on the pressure only. Such methods are common in the simulation of injection mold flow in the plastic industry.

The present work is to simulate flows in quasi-cylindrical domain by a projection on polynomial spaces and to recover the Hele-Shaw approximation with the spaces spanned by their lowest order polynomials. Moreover, one can simulate 3D features of flows (like vortices in the thickness) by increasing the degree of the approximation spaces, thus extending the classical Hele-Shaw model.

1.1 Definition of the problem

A quasi-cylindrical domain is a N-dimensional domain Ω such that there exists a $(N-1)$-dimensional domain ω and two real-valued lipschitz functions h^+ and h^- on ω with $h^-(x_\omega) < h^+(x_\omega)$ for all $x_\omega = (x_1,\ldots,x_{N-1}) \in \omega$:

$$\Omega = \{(x_\omega, x_N) \,|\, x \in \omega \text{ and } y \in [h^-(x_\omega), h^+(x_\omega)]\} \subset \mathbf{R}^3 \quad (1)$$

Hence, the functions h^+ and h^- describe the shape of the upper and lower surfaces of the domain, and the flow occurs between these two surfaces. Following an idea of Vogelius-Babuska (see **?**), **?**), **?**)) one takes advantage of the quasi-cylindrical shape of Ω to project the N-dimensional Stokes problem on a $(N-1)$-dimensional problem set on ω.

Let a mapping

$$T: \begin{array}{ccc} \Omega & \longrightarrow & \hat\Omega \\ (x_\omega, x_N) & \longmapsto & (\hat x_\omega = x_\omega, \hat x_N) \end{array}$$

be such that $\hat\Omega$ is the cylindrical domain $\omega \times [-1,1]$. Hence,using this mapping, one reformulates the Stokes problem onto $\hat\Omega$ and approximates the new problem by projecting the pressure and velocity on the spaces

$$\begin{aligned} Q_J &= \{q \in L^2(\hat\Omega)/\exists (q_j)_{j=0..J} \in L^2(\omega); \\ &\quad q = \sum_{j=0}^{J} q_j(x_\omega)\psi_j(x_N)\} \\ V_J &= \{\mathbf{v} \in H^1(\hat\Omega)^N/\exists (\mathbf{v}_j)_{j=0..J} \in H_0^1(\omega)^N; \\ &\quad \mathbf{v} = \sum_{j=0}^{J} \mathbf{v}_j(x_\omega)\varphi_j(x_N)\} \end{aligned}$$

[1] Laboratoire d'Analyse Numérique, Tour 55-56, 5^e étage, Université Pierre & Marie Curie, 4 place Jussieu, 75252 Paris Cedex 05. E-mail: ricou@ann.jussieu.fr

[2] Institute of Computer Science, The Hebrew University, Jerusalem 91904, Israel (on leave at DER Falcult Lonard de Vinci, Paris la Dfense, France). E-mail: berco@cs.huji.ac.il

where ψ_j and φ_j are given polynomials. Define these polynomials such that the Inf-Sup condition (cf **?**)) is enforced on the Stokes equations projected onto V_J and Q_J. This will ensure that the reduced problem is well posed. It can be shown then that the solution of this reduced problem converges to the solution of the original Stokes equations as the degree of the polynomials tends to infinity.

The reduced problem can be discretised by a finite element method in the x_ω direction. Thus, the N-dimension Stokes problem is computed on a $(N-1)$-dimension mesh. This leads to the definition of elements for which the final problem is well posed.

The stiffness matrix obtained is block defined and smaller than the stiffness matrix one would have with a 3D FEM for the same quality of result. Hence, the time computation is reduced by taking advantage of its special shape (and adapted preconditionners).

Results are compared with the Hele-Shaw model and the full dimension F.E.M.. On one hand, the method of reduction is more accurate than the Hele-Shaw model (it recovers this model at its lower degree of approximation). On this other hand, this method is cheaper than a full dimension F.E.M.. Finally, this is confirmed by numerical examples.

2 The dimensional reduction

All the results not detailed here can be found in the book of **?**) and **?**).

Let Ω be a quasi-cylindrical domain ($N = 2, 3$)

$$\Omega = \{(x_\omega, x_N) \,|\, x \in \omega \text{ and } y \in [h^-(x_\omega), h^+(x_\omega)]\} \subset \mathbf{R}^N \tag{2}$$

where $h^-(x_\omega)$ and $h^+(x_\omega)$ are two lipschitz real-value functions defining the thickness of the domain ($h^-(x_\omega) < h^+(x_\omega)$). Assume that the upper and lower surfaces $\Gamma_H = \{(x_\omega, x_N) | x \in \omega, y = h^-(x_\omega) \text{ or } h^+(x_\omega)\}$ are walls (of a mold cavity for example), the boundary conditions used are no-slip boundary conditions. The "vertical" borders, $\Gamma_V = \{(x_\omega, x_N) | x_\omega \in \partial\omega, y \in [h^-(x_\omega), h^+(x_\omega)]\} = \Gamma_D + \Gamma_N$, will be walls, inflow, outflow or free boundaries.

Let $\mathbf{u}(x_\omega, x_N)$ and $p(x_\omega, x_N)$ be the velocity of the flow and the fluid pressure at point $(x_\omega, x_N) \in \Omega$, respectively. The flow is governed by the Stokes equations with mixed

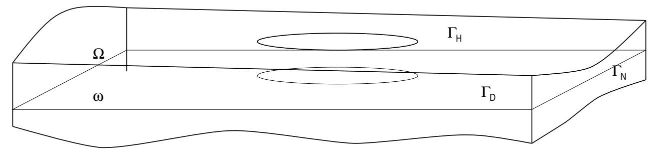

Figure 1 : a quasi-cylindrical domain

Neumann-Dirichlet boundary conditions i.e. it is the solution of the problem: Find $(\mathbf{u}, p) \in H^1(\Omega)^N \times L^2(\Omega)$ such that

$$\left\{ \begin{array}{rll} -\nu\Delta\mathbf{u} + \nabla p & = \mathbf{f} & \text{on } \Omega \\ \nabla.\mathbf{u} & = 0 & \\ \mathbf{u} & = \mathbf{0} & \text{on } \Gamma_H \\ \mathbf{u} & = \mathbf{g} & \text{on } \Gamma_D \\ -\nu\frac{\partial\mathbf{u}}{\partial\mathbf{n}} + p.\mathbf{n} & = \mathbf{0} & \text{on } \Gamma_N \end{array} \right. \tag{3}$$

with $\mathbf{f} \in L^2(\Omega)^N$ and $\mathbf{g} \in H^{1/2}(\Gamma)$.

Proposition 2.1 *The Stokes problem with mixed boundary conditions (3) has a solution. This solution* $(\mathbf{u}, p)$ $\in H^1(\Omega)^N \times L^2(\Omega)$ *is unique.*

Proof This proposition is a variation of known results. A proof is proposed in appendix A. $\diamond$

The weak formulation of the Stokes problem is

$$\left\{ \begin{array}{lll} \nu \displaystyle\int_\Omega \nabla\mathbf{u}\nabla\mathbf{v}\, dx_\omega\, dx_N - & \int_\Omega p\nabla.\mathbf{v}\, dx_\omega\, dx_N & \\ & = \displaystyle\int_\Omega \mathbf{f}\mathbf{v}\, dx_\omega\, dx_N & \forall\mathbf{v} \in V \\ -\displaystyle\int_\Omega \nabla.\mathbf{u}\, q\, dx_\omega\, dx_N & = \quad 0 & \forall q \in Q \end{array} \right. \tag{4}$$

also written

$$\left\{ \begin{array}{rcll} a(\mathbf{u}, \mathbf{v}) + b(\mathbf{v}, p) & = & <\mathbf{f}, \mathbf{v}>_{V' \times V} & \forall\mathbf{v} \in V \\ b(\mathbf{u}, q) & = & 0 & \forall q \in Q \end{array} \right. \tag{5}$$

with $a(\mathbf{u}, \mathbf{v}) = \nu \displaystyle\int_\Omega \nabla\mathbf{u}\nabla\mathbf{v}\, dx_\omega\, dx_N$ and $b(\mathbf{v}, p) = -\displaystyle\int_\Omega p\nabla.\mathbf{v}\, dx_\omega\, dx_N$.

Let us apply the bijective mapping T to the Stokes problem

$$\begin{array}{rccl} T: & \Omega & \longrightarrow & \hat{\Omega} = \omega \times [-1, 1] \\ & (x_\omega, x_N) & \longmapsto & (\hat{x}_\omega = x_\omega, \hat{x}_N) \end{array} \tag{6}$$

where

$$\hat{x}_N(x_\omega, x_N) = \frac{1}{h^+(x_\omega) - h^-(x_\omega)}(2x_N - h^+(x_\omega) - h^-(x_\omega)). \tag{7}$$

Hence the new problem is: Find $(\hat{\mathbf{u}}, \hat{p}) \in \hat{V} \times \hat{Q}$ such that

$$\left\{ \begin{array}{ll} \nu \int_{\hat{\Omega}} (\nabla T \hat{\nabla}) \hat{\mathbf{u}} \, (\nabla T \hat{\nabla}) \hat{\mathbf{v}} |\nabla T^{-1}| \, d\hat{x}_\omega d\hat{x}_N & \\ \quad - \int_{\hat{\Omega}} \hat{p} \, (\nabla T \hat{\nabla}).\hat{\mathbf{v}} |\nabla T^{-1}| \, d\hat{x}_\omega d\hat{x}_N & \\ \quad = \int_{\hat{\Omega}} \hat{\mathbf{l}} \hat{\mathbf{v}} |\nabla T^{-1}| \, d\hat{x}_\omega d\hat{x}_N & \forall \hat{\mathbf{v}} \in \hat{V} \\ - \int_{\hat{\Omega}} (\nabla T \hat{\nabla}).\hat{\mathbf{u}} \, \hat{q} |\nabla T^{-1}| \, d\hat{x}_\omega d\hat{x}_N = 0 & \forall \hat{q} \in \hat{Q} \end{array} \right. \tag{8}$$

also written

$$\left\{ \begin{array}{rcll} \hat{a}(\hat{\mathbf{u}}, \hat{\mathbf{v}}) + \hat{b}(\hat{\mathbf{v}}, \hat{p}) & = & < \hat{\mathbf{l}}, \hat{\mathbf{v}} >_{\hat{V}' \times \hat{V}} & \forall \hat{\mathbf{v}} \in \hat{V} \\ \hat{b}(\hat{\mathbf{u}}, \hat{q}) & = & 0 & \forall \hat{q} \in \hat{Q} \end{array} \right. \tag{9}$$

The new spaces are $\hat{V} = \hat{H}^1(\hat{\Omega})^N$ and $\hat{Q} = L^2(\hat{\Omega})$ where:

$$\hat{H}^1(\hat{\Omega}) = \left\{ \hat{\mathbf{v}} \in L^2(\hat{\Omega})^N \text{ s.t. } \tilde{\nabla} \hat{\mathbf{v}} \in L^2(\hat{\Omega})^N \right\} \tag{10}$$

$$\text{with } \tilde{\nabla} = (\nabla T \hat{\nabla}) = \begin{pmatrix} \dfrac{\partial}{\partial \hat{x}_\omega} + \dfrac{\partial \hat{x}_N}{\partial x_\omega} \dfrac{\partial}{\partial \hat{x}_N} \\ \dfrac{\partial \hat{x}_N}{\partial x_N} \dfrac{\partial}{\partial \hat{x}_N} \end{pmatrix} \tag{11}$$

where

$$\begin{array}{rcl} \dfrac{\partial \hat{x}_N}{\partial x_\omega} & = & \dfrac{-1}{h^+ - h^-} \left(\left(\dfrac{\partial h^+}{\partial x_\omega} + \dfrac{\partial h^-}{\partial x_\omega} \right) + \left(\dfrac{\partial h^+}{\partial x_\omega} - \dfrac{\partial h^-}{\partial x_\omega} \right) \hat{x}_N \right) \\ & = & H(x_\omega) + G(x_\omega) \, \hat{x}_N, \\ \dfrac{\partial \hat{x}_N}{\partial x_N} & = & \frac{2}{h^+ - h^-}. \end{array} \tag{12}$$

Since $h^-(x_\omega)$ and $h^+(x_\omega)$ are two lipschitz functions, and since $h^+(x_\omega) > h^-(x_\omega)$, and ω is a bounded set, these two derivatives are bounded. Therefore $\hat{H}^1(\hat{\Omega}) = H^1(\hat{\Omega})$.

Proposition 2.2 *The problem with mixed boundary conditions (8) has a solution. This solution* $(\hat{\mathbf{u}}, \hat{p}) \in H^1(\hat{\Omega})^N \times L^2(\hat{\Omega})$ *is unique.*

Proof The transformation T is a bilipschitz homeomorphism. Since problem (3) has a unique solution, the problem reformulated (8) using this transformation has also a unique solution in $T(V(\Omega)) \times T(Q(\Omega)) = H^1(\hat{\Omega}) \times L^2(\hat{\Omega})$. $\diamond$

Now that the problem is defined on $\hat{\Omega} = \omega \times [-1, 1]$, the idea is to approximate the solutions $\hat{\mathbf{u}}$ and $\hat{p}$ by functions that are polynomial with respect to $\hat{x}_N$ (the thickness). Let

$$\hat{\mathbf{u}}(\hat{x}_\omega, \hat{x}_N) = \sum_{j=0}^{J} \hat{\mathbf{u}}_{\mathbf{j}}(\hat{x}_\omega) \varphi_j(\hat{x}_N), \tag{13}$$

$$\hat{p}(\hat{x}_\omega, \hat{x}_N) = \sum_{j=0}^{J} \hat{p}_j(\hat{x}_\omega) \psi_j(\hat{x}_N), \tag{14}$$

where φ_j and ψ_j are polynomials defined on $[-1, 1]$ and $\hat{\mathbf{u}}_{\mathbf{j}}(\hat{x}_\omega)$ and $\hat{p}_j(\hat{x}_\omega)$ $(\hat{x} \in \omega)$ the coefficients of the projection of $\hat{\mathbf{u}}$ and $\hat{p}$ on these polynomials. Furthermore the boundary conditions on $\hat{x}_N = \pm 1$, which are still Dirichlet homogeneous ones, have to be satisfied.

The polynomials φ_j and ψ_j must satisfy three conditions: the reduced problem must be well defined, the Hele-Shaw approximation should be recovered and there should be some L^2-orthogonality to reduce the numerical cost of the simulation.

Let ψ_j be the Legendre polynomials:

$$\begin{array}{ll} \psi_j(y) = L_j(y) & \text{with } L_j \text{ the Legendre polynomials of order } j: \\ & L_0 = 1, \; L_1 = y, \\ & L_j = (y - \lambda_j) L_{j-1}(y) - \mu_j L_{j-2}(y) \end{array} \tag{15}$$

where $\lambda_j = \dfrac{||L_{j-1}||^2}{||L_{j-2}||^2}$ and $\mu_j = \dfrac{(yL_{j-1}, L_{j-1})}{||L_{j-2}||^2}$.

They define an orthogonal basis of $L^2(-1, 1)$ for its usual scalar product. Furthermore $\psi_0 = 1$ which means that the pressure over the thickness will be constant at the lowest degree of approximation. This is similar to the Hele-Shaw approximation (see 32).

The polynomials φ_j are defined by

$$\varphi_j = \psi_j - \psi_{j+2}, \qquad \varphi_j \text{ is of degree } j+2. \tag{16}$$

Here again, the first polynomial φ_0 recover the typical parabolic profile of the velocity for Hele-Shaw flows.

With these definitions, one can check that the reduced problem is well defined.

Let $w:(-1,1)\to\mathbf{R}_+$ be a weight function and let

$$L^2_w(-1,1) \;:=\; \{v:(-1,1)\to\mathbf{R}\,|\,v \text{ is measurable and } ||v||_{0,w}<\infty\}$$

where $||v||_{0,w}$ is the norm induced by the scalar product

$$(u,v)_w := \int_{-1}^{1} u(y)\,v(y)\,w(y)\,dy.$$

Proposition 2.3 *The set of polynomials $(\varphi_j)_{j\geq 0}$ is an orthogonal basis of the space $L^2_w(-1,1)$ for the weight $w(y)=\dfrac{1}{1-y^2}$.*

Proof: Notice that the space $(1-y^2)\mathbf{P}$ is dense in $L^2_w(-1,1)$ for the L^2_w-norm.

Since the Legendre polynomials verify $\psi_j(1)=1$ and $\psi_j(-1)=(-1)^j$, $\varphi_j(\pm 1)=0$. Therefore $\varphi_j(y)=(1-y^2)\tilde\varphi_j(y)$ where $\tilde\varphi_j(y)$ is a polynomial of degree j, and the family $(\varphi_j)_{j=0..J}$ is a basis of $(1-y^2)\mathbf{P}_J$.

The orthogonality of the polynomials φ_j for the scalar product of $L^2_w(-1,0)$ is satisfied if $(\varphi_i,\varphi_j)_w=0$ for all $i<j\leq J$.

$$\begin{aligned}(\varphi_i,\varphi_j)_w &= \int_{-1}^{1}(1-y^2)\tilde\varphi_i(y)\,\varphi_j(y)\,\frac{1}{1-y^2}\,dy\\ &= \int_{-1}^{1}\tilde\varphi_i(y)\,(\psi_j-\psi_{j+2})(y)\,dy,\end{aligned}$$

The polynomial $\tilde\varphi_i\in\mathbf{P}_i$ and therefore is a linear combination of the $(i+1)$ first Legendre polynomials. Consequently

$$\begin{aligned}(\varphi_i,\varphi_j)_w &= \int_{-1}^{1}\left(\sum_{k=0}^{i}\tilde\varphi_{ik}\psi_k(y)\right)(\psi_j-\psi_{j+2})(y)\,dy\\ &= 0 \qquad \text{since } i<j.\end{aligned}$$

$\diamond$

Hence the space spanned by the φ_j is dense in $H^1_0(-1,1)$ since $H^1_0(-1,1)=L^2_w(-1,1)\cap H^1(-1,1)$.

One can also remark the φ_j are orthogonal for the semi-norm in $H^1(-1,1)$ and that

$$\int_{-1}^{1}\varphi'_j\,\psi_i\,dy = 0 \;\text{ for } i\neq j-1$$

since $\varphi'_j=-(2j+3)\psi_{j+1}$.

2.1 Discretization in the thickness

Note: From now on, $w(y)$ denotes the weight $\dfrac{1}{1-y^2}$. The functions ψ_j and φ_j are the one defined by (15) and (16).

$$\begin{aligned}\text{Let } Q_J &= \{q\in L^2(\hat\Omega)/\exists(q_j)_{j=0..J}\in L^2(\omega);\\ &\qquad q=\sum_{j=0}^{J}q_j(x_\omega)\psi_j(x_N)\}\\ V_J &= \{\mathbf{v}\in H^1(\hat\Omega)^N/\exists(\mathbf{v}_j)_{j=0..J}\in H^1_{0,\gamma_D}(\omega)^N;\\ &\qquad \mathbf{v}=\sum_{j=0}^{J}\mathbf{v}_j(x_\omega)\varphi_j(x_N)\}\,.\end{aligned}$$

Proposition 2.4 $\displaystyle\bigcup_{J=0}^{\infty}V_J$ *is dense in $\hat V$.*

Proof: A proof is proposed in appendix A.

Proposition 2.5 $\displaystyle\bigcup_{J=0}^{\infty}Q_J$ *is dense in $\hat Q$.*

Proof: Apply the same proof as above to the series q^J in L^2. $\diamond$

To conclude, given $J<\infty$ the transformed Stokes problem (9) can be discretised as follows: find $(\mathbf{u}^J,p^J)\in V_J\times Q_J$ such that

$$\left\{\begin{array}{rcll}\hat a(\mathbf{u}^J,\mathbf{v}^J)+\hat b(\mathbf{v}^J,p^J) &=& <\hat{\mathbf{f}},\mathbf{v}^J>_{V'_J\times V_J} & \forall\mathbf{v}^J\in V_J\\ \hat b(\mathbf{u}^J,p^J) &=& 0 & \forall q^J\in Q_J\end{array}\right. \tag{17}$$

Proposition 2.6 *The reduced Stokes problem (17) has a solution ($\mathbf{u}^J,p^J$). This solution is unique in $V_J\times Q_J$.*

Proof: A proof is given in appendix A.

Remark 2.1 *Note that equation (48) gives an unconditional stability of the dimension reduction : the Inf-Sup coefficient β is not linked to the dimension J of the polynomial space V^J. This is not the case for 2D spectral elements (see* **?***)).*

To complete the reduction of the probleme, one has to analyze the convergence of the reduced problem when $J\to\infty$.

It is shown in **?**), that the discretization error for an abstract problem of the form (17) is given by

$$||\mathbf{u}^J - \hat{\mathbf{u}}||_{\hat{V}} \leq c_1 \inf_{\mathbf{v}^J \in V_J} ||\hat{\mathbf{u}} - \mathbf{v}^J||_{\hat{V}} + c_2 \inf_{q^J \in Q_J} ||p - q^J||_{\hat{Q}} \quad (18)$$

$$\begin{aligned} ||p^J - \hat{p}||_{\hat{Q}/Ker(Div)} &\leq (1 + \frac{||\hat{b}||}{k_J}) \inf_{q^J \in Q_J} ||q^J - \hat{p}||_{\hat{Q}} \\ &+ \frac{||\hat{a}||}{\beta} ||\hat{\mathbf{u}} - \mathbf{u}^J||_{\hat{V}} \end{aligned} \quad (19)$$

with

$$\begin{aligned} c_1 &\leq (1 + \frac{||\hat{a}||}{\alpha})(1 + \frac{||\hat{b}||}{\beta}) \\ c_2 &\leq \frac{||\hat{b}||}{\alpha} \end{aligned}$$

where α is the ellipticity constant and β the constant of the Inf-Sup condition.

Let Π_J be the operator of $L^2(-1,1)$ orthogonal projection onto $\mathbf{P}_J(-1,1)$. Under the following assumption of regularity: $u \in H^m(-1,1) \cap H_0^1(-1,1)$ and $q \in H^n(-1,1)$, we have (see **?**)):

$$||p - \Pi_J p||_0 \leq C(n)\, J^{-n} ||p||_n \quad n \geq 0 \quad (20)$$

$$|u - \Pi_J^{1,0} u|_1 \leq C(m)\, J^{1-m} ||u||_m \quad m \geq 1 \quad (21)$$

Unfortunately, in our case, $\mathbf{u}$ is in $H_0^1(-1,1)^N$ and q in $H^0(-1,1)$. This is insufficient to obtain an estimate of the error by $C_1(J)||\mathbf{u}||_1 + C_2(J)||q||_0$ with $C_i(J) \underset{J\to\infty}{\longrightarrow} 0$. So the error analysis does not prove by itself that the solution $(\mathbf{u}^J, p^J)$ of the reduced problem will converge to the solution $(\mathbf{u}, p)$ of the continuous problem when $J \to \infty$. However the following theorem gives the convergence:

Theorem 2.1 *The solution $(\mathbf{u}^J, p^J)$ of the reduced Stokes problem (17) converges to the solution $(\hat{\mathbf{u}}, \hat{p})$ of the continuous problem (8) when $J \to \infty$.*

Proof: Due to propositions (2.4) and (2.5)

$$\lim_{J\to\infty} \inf_{\mathbf{v}^J \in V_J} ||\hat{\mathbf{u}} - \mathbf{v}^J||_V = 0$$

$$\lim_{J\to\infty} \inf_{q^J \in Q_J} ||\hat{p} - q^J||_Q = 0.$$

Therefore the convergence is achieved with (18) and (19). ◇

This implies that the solution $(T^{-1}(\mathbf{u}^J), T^{-1}(p^J))$ converges to the continuous Stokes problem (3).

All this error analysis has been done for the worst case, and without taking in account the shape of the domain or the regularity of the second member. It is known that with hypothesis on the domain (convex, polygonal...) the solution is more regular: $(\mathbf{u}, p) \in H^{1+s}(\Omega)^N \times H^s(\Omega) with s > 0$ (see **?**)). This, combined with the fact that the influence of corners on the regularity of a Stokes flow is local, explain why the numerical results show a faster convergence than expected from the results above.

3 Discretization of the problem over ω

From now on, $\mathbf{u}$ denotes the solution of the reduced problem (17), formerly called $\mathbf{u}^J$, and not the solution of the original problem (3) anymore. The same is done with p so that: $(\mathbf{u}, p) \in V_J \times Q_J$.

The purpose is now to discretize the reduce problem with a finite element method, hence to have a usual finite element method with its advantages but applied on a domain of $N-1$ dimensions.

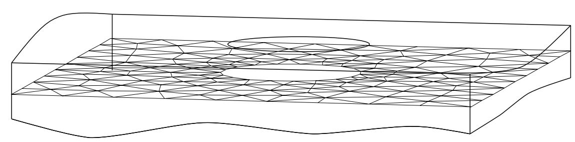

Figure 2 : Finite element mesh on ω

Let $V_{Jh} \hookrightarrow V_J$ and $Q_{Jh} \hookrightarrow Q_J$ be finite dimensional subspaces of V_J and Q_J respectively (the subscript h refers to the size of the mesh elements). The discretized problem is: Find $(\mathbf{u}_h, p_h) \in V_{Jh} \times Q_{Jh}$ such that:

$$\left\{ \begin{array}{rcll} \hat{a}(\mathbf{u}_h, \mathbf{v}_h) + \hat{b}(\mathbf{v}_h, p_h) &=& < \mathbf{f}_h, \mathbf{v}_h >_{V' \times V} & \forall \mathbf{v}_h \in V_{Jh} \\ \hat{b}(\mathbf{u}_h, q_h) &=& 0 & \forall q_h \in Q_{Jh} \end{array} \right. \quad (22)$$

Proposition 3.1 *Under the assumption the Inf-Sup condition is satisfied for the chosen element, the discretized problem (22) has a unique solution $(\mathbf{u}_h, p_h) \in V_{Jh} \times Q_{Jh}$.*

The proof is standard (see **?**)).

3.1 The elements

To complete the discretization, one has to define a finite element which satisfies the Inf-Sup condition for the discrete reduced problem (22).

This means, if Π_h is the interpolation operator, it has to be such that

$$b(\Pi_h \mathbf{u} - \mathbf{u}, q_h) = 0 \quad \forall q_h \in Q_{Jh} \tag{23}$$

$$||\Pi_h \mathbf{u}||_{V_J h} \leq C\, ||\mathbf{u}||_{V_J} \tag{24}$$

with

$$\begin{aligned} & b(\Pi_h \mathbf{u}_j - \mathbf{u}_j, q_{hj}) \\ & \quad = \sum_{i=1}^{N} \left(C_1 \int_\omega \frac{\partial}{\partial x_\omega} (\Pi_h u_{ij} - u_{ij})\, q_{hj}\, dx_\omega \right. \\ & \qquad + C_2 \int_\omega H(x_\omega)\, (\Pi_h u_{ij} - u_{ij})\, q_{hj}\, dx_\omega \\ & \qquad \left. + C_3 \int_\omega G(x_\omega)\, (\Pi_h u_{ij} - u_{ij})\, q_{hj}\, dx_\omega \right) \\ & \quad + C_2 \int_\omega \frac{\partial \hat{x}_N}{\partial x_N} (\Pi_h u_{Nj} - u_{Nj})\, q_{hj}\, dx_\omega \end{aligned}$$

where $C_1 = \int_{-1}^{1} \varphi_j \psi_k\, d\hat{x}_N$, $C_2 = \int_{-1}^{1} \varphi'_j \psi_k\, d\hat{x}_N$ and $C_3 = \int_{-1}^{1} \varphi'_j \psi_k\, \hat{x}_N\, d\hat{x}_N$.

The first part of the linear constraint b is the divergence constraint in the reduced dimension. It will be null if the chosen element is a good element for the regular Stokes problem on ω. If we use a piecewise constant pressure, the easiest way to nullify the others integrals is to have a degree of freedom inside the element, i.e. to have "bubble" function – $H(x_\omega), G(x_\omega)$ and $\partial \hat{x}_N / \partial x_N$ are known functions –. Hence the P1-bubble/P0 element satisfies the Inf-Sup condition.

The second condition (24) is satisfied if the interpolation operator is such that $\Pi_h p_k = p_k$ for all polynomial defined onto the element K: $p_k \in \mathbf{P}_k(K)$.

Example: the P2/P0 element. This element satisfies the Inf-Sup condition for the Stokes problem in 2D, therefore the first integral vanishes.

One has to define the Π_h operator on u_3 such that the last integrals are null i.e. such that

$$\begin{aligned} \int_K \Pi_h u_3\, dx_\omega \quad = \quad & \int_K u_3\, dx_\omega - \sum_{i=1}^{2} \int_K (H(x_\omega) \\ & + \frac{C_3}{C_2} G(x_\omega))\, (\Pi_h u_{ij} - u_{ij})\, dx_\omega \end{aligned} \tag{25}$$

Let $\Pi_h u_3(M_i) = u_3(M_i)$ where M_i are the nodes on the vertices of K and M_{ij} on its edges. Hence the three degree of freedom $\Pi_h u_3(M_{ij})$ stay free. One has to be fix to satisfy (25), therefore 2 remain free. They will be used by other elements, so that we can keep the conformity *if* there are more free edges than elements. ∘

As in the 2D Stokes problem, the Q1/Q0 element can give good numerical result even if it does not satisfy the Inf-Sup condition. We used it for the examples.

3.2 The matrix system

The resulting stiffness matrix is block defined: each usual block for each degree of freedom (u_x, u_y, u_z, p) is subdivided in $(J+1) \times (J+1)$ blocks of the same shape. Thanks to the orthogonalities of φ_j and ψ_j, and according to the shape of two surfaces h^+ and h^-, some of these blocks are null.

For example the laplacian gives a pentadiagonal block defined matrix and the equation of the mass conservation $(\nabla.\mathbf{u} = 0)$ leads to the following shape (for $J = 4$) :

$$\begin{pmatrix} * & 0 & 0 & 0 & 0 & 0 & 0 & 0 & 0 & 0 \\ * & * & 0 & 0 & 0 & * & 0 & 0 & 0 & 0 \\ * & * & * & 0 & 0 & 0 & * & 0 & 0 & 0 \\ 0 & * & * & * & 0 & 0 & 0 & * & 0 & 0 \\ 0 & 0 & * & * & * & 0 & 0 & 0 & * & 0 \end{pmatrix} \begin{pmatrix} \mathbf{u}_{1,0} \\ \mathbf{u}_{1,1} \\ \mathbf{u}_{1,2} \\ \mathbf{u}_{1,3} \\ \mathbf{u}_{1,4} \\ \mathbf{u}_{2,0} \\ \vdots \\ \mathbf{u}_{2,4} \end{pmatrix} = \begin{pmatrix} 0 \end{pmatrix} \tag{26}$$

where the stars are for non zero matrices. This shape comes from the following matrices of coefficients :

$$\left(\int_{-1}^{1}\psi_i\varphi_j\,d\xi\right)_{ij} = \begin{bmatrix} 2 & 0 & 0 & 0 & 0 \\ 0 & 2/3 & 0 & 0 & 0 \\ -2/5 & 0 & 2/5 & 0 & 0 \\ 0 & -2/7 & 0 & 2/7 & 0 \\ 0 & 0 & -2/9 & 0 & 2/9 \end{bmatrix}, \quad (27)$$

$$\left(\int_{-1}^{1}\psi_i\frac{\partial\varphi_j}{\partial\xi}\,d\xi\right)_{ij} = \begin{bmatrix} 0 & 0 & 0 & 0 & 0 \\ -2 & 0 & 0 & 0 & 0 \\ 0 & -2 & 0 & 0 & 0 \\ 0 & 0 & -2 & 0 & 0 \\ 0 & 0 & 0 & -2 & 0 \end{bmatrix}, \quad (28)$$

$$\left(\int_{-1}^{1}\psi_i\frac{\partial\varphi_j}{\partial\xi}\,\xi\,d\xi\right)_{ij} = \begin{bmatrix} -2 & 0 & 0 & 0 & 0 \\ 0 & -4/3 & 0 & 0 & 0 \\ -4/5 & 0 & -6/5 & 0 & 0 \\ 0 & -6/7 & 0 & -8/7 & 0 \\ 0 & 0 & -8/9 & 0 & -10/9 \end{bmatrix} \quad (29)$$

Here is the shape of the matrix of the 2D+1 [3] examples proposed in the end of this paper :

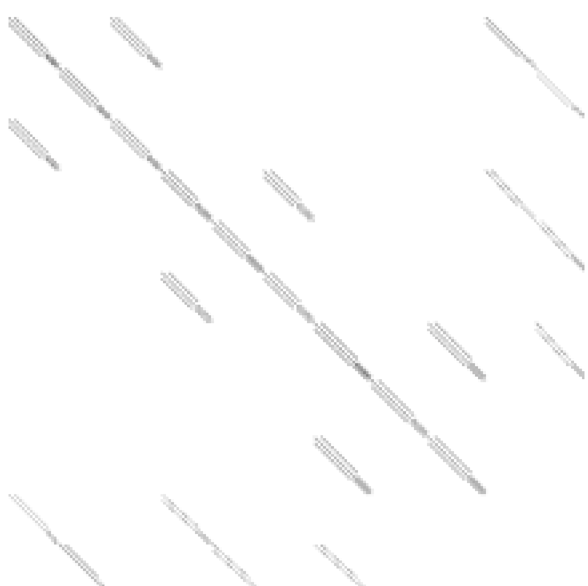

Figure 3 : stiffness matrix of a 2D+1 example

The stiffness matrix is smaller than the one we would get from a finite element method applied on the original problem if the number of polynomial function needed is smaller than the number of node needed in the thickness for the FEM to get the same result. One can show that, for iterative solvers, the reduction method is advantageous if the ratio number of node, number of function needed is more the 1.5. It seems reasonable to accept that this value is under reality (the ratio of the proposed examples is around 3).

The speed of computation can be increased with preconditionners for iterative methods. Computation have shown that a good choice for the Uzawa algorithm is an incomplete Choleski factorization on each diagonal bloc for the computation of the speed, and a incomplete Choleski factorization of the matrix defined by the operator $\frac{1}{\beta}\hat{\Delta}$ where $\hat{\Delta} = \hat{\nabla}.\hat{\nabla}$ (see eq.(11)) and $\beta = (\frac{\partial\hat{y}}{\partial x_\omega})^2 + (\frac{\partial\hat{y}}{\partial x_N})^2$.

Here are some CPU time of 2D and 3D computations with or without the dimensional reduction method, with the number of function in the first case and the number of nodes used in the thickness in the second one [4]:

	with reduction	without (F.E.M.)
a 2D example	8s, 1 function 22s, 3 functions	11s, 5 nodes 49s, 9 nodes
a 3D example	612s, 1 function 4509s, 3 functions	12813s, 5 nodes 33378s, 9 nodes

Figure 4 : Examples of CPU time according to the method and precision

The right number of node to have similar result is not always easy to find since one method can give better results for some criteria, and worst for other. Hence, we have to arbitrary decide when results with and without reduction are similar. However, the differences of CPU time are large enough to show the acceleration due to the reduction method.

4 Comparaison with the Hele-Shaw approximation

The most common approximation for low Reynolds flows between two close plates (N=3) is the Hele-Shaw approximation.

[3] 2D+1 computations have a 3D domain and variables but, by the use the reduction method, compute the solution on a 2D mesh.

[4] The values of the time computation are not important by themselves, but compared to the others. The solver is the same as far as possible for the two methods.

4.1 The Hele-Shaw approximation

The name of the Hele-Shaw flow comes from experiments Hele-Shaw has published in Nature in 1898 (see **?**)). He noticed then, that a flow between two plates becomes laminar when the two plates are close enough (see also **?**), **?**)).

The features of Hele-Shaw flows and the governing equations (taken form the manual of the software Moldflow, **?**)) come from estimates of the order of magnitude of each term of the equations. In order to compare this orders of magnitude, one need to define characteristic values (length of the domain, thickness, fluid viscosity, density...), to assume that the fluid is some melt fluid and that the ratio between the thickness and the length is small compared to the unity. Therefore the momentum conservation equation leads to the following equations:

$$\frac{\partial p}{\partial x_1} = \frac{\partial}{\partial x_3}\left(\mu\frac{\partial u_1}{\partial x_3}\right), \tag{30}$$

$$\frac{\partial p}{\partial x_2} = \frac{\partial}{\partial x_3}\left(\mu\frac{\partial u_2}{\partial x_3}\right), \tag{31}$$

$$\frac{\partial p}{\partial x_3} = 0, \tag{32}$$

where now the direction of the thickness is the x_3 direction.

Integrating these equations over the thickness, and assuming this thickness is delimited by $+h$ and $-h$, one can see that the velocity profile is parabolic:

$$u_1(x_3) = \alpha(x_3^2 - h),\ u_y(x_3) = \beta(x_3^2 - h),\ u_3 = 0. \tag{33}$$

More precisely, the velocities are:

$$u_x(x_1,x_2,x_3) = -\frac{1}{2\mu}\frac{\partial p}{\partial x_1}(x_1,x_2)\,(x_3^2 - h), \tag{34}$$

$$u_y(x_1,x_2,x_3) = -\frac{1}{2\mu}\frac{\partial p}{\partial x_2}(x_1,x_2)\,(x_3^2 - h), \tag{35}$$

$$u_z(x_1,x_2,x_3) = 0. \tag{36}$$

The flow is governed by the pressure gradient, and the pressure can be obtain from the mass conservation equation:

$$\frac{\partial}{\partial x_1}\left(S\frac{\partial p}{\partial x_1}\right) + \frac{\partial}{\partial x_2}\left(S\frac{\partial p}{\partial x_2}\right) = 0 \tag{37}$$

where $S(x_1,x_2)$ is a scalar function of the upper and lower boundaries and of the viscosity. This function is constant when the boundaries are two parallel planes and the viscosity is constant.

4.2 Comparaison between the two methods

Proposition 4.1 *The Hele-Shaw approximation and the reduction method at its lower degree ($V_J = V_0$ and $Q_J = Q_0$) are similar.*

Proof: In the reduction method, the mass conservation equation becomes:

$$\left(\frac{\partial u_{1,0}}{\partial x_1} + \frac{\partial u_{2,0}}{\partial x_2}\right)(x_1,x_2)\,\varphi_0(x_3) + u_{3,0}(x_1,x_2)\,\frac{\partial \varphi_0}{\partial x_3}(x_3) = 0 \qquad \forall x_3 \in [-1,1]. \tag{38}$$

Hence

$$\frac{\partial u_{1,0}}{\partial x_1} + \frac{\partial u_{2,0}}{\partial x_2} = 0 \tag{39}$$

$$\text{and} \quad u_{3,0} = 0 \tag{40}$$

The momentum conservation equation gives:

$$\mu\left(\left(\frac{\partial^2 u_{1,0}}{\partial x_1^2} + \frac{\partial^2 u_{1,0}}{\partial x_2^2}\right)\varphi_0 + u_{1,0}\frac{\partial^2 \varphi_0}{\partial x_3^2}\right) = \frac{\partial p}{\partial x_1}\psi_0, \tag{41}$$

the same in x_2 and $0 = 0$ in x_3 which is consistent ($\psi_0 = 1$).

Since this equation is true for all x_3, and because $\frac{\partial^2\varphi_0}{\partial x_3^2}$ and ψ_0 are constant, $\varphi_0(x_3)$ stays the only term varying with x_3 thus

$$\frac{\partial^2 u_{1,0}}{\partial x_1^2} + \frac{\partial^2 u_{1,0}}{\partial x_2^2} = 0. \tag{42}$$

Therefore, by integrating the momentum equation over x_3

$$u_{1,0} = \frac{1}{\mu C_1}\frac{\partial p}{\partial x_1}, \tag{43}$$

$$u_{2,0} = \frac{1}{\mu C_2}\frac{\partial p}{\partial x_2}. \tag{44}$$

Since $\mathbf{u} = \mathbf{u}_0\,\varphi_0$, the reduction method at its lower degree recovers indeed the Hele-Shaw approximation. ⋄

Remark 4.1 *Note that any set of polynomial functions like $(1-y^2)\,f_j$, with f_j of degree j instead of the φ_j would have also recovered the Hele-Shaw approximation. The main advantage of the φ_j is their orthogonality for the H^1 semi-norm which reduce the cost of the computation.*

Remark 4.2 *When the Hele-Shaw approximation is not anymore valid – if the distance between the two borders is too important, the borders are too irregular, the viscosity is non-Newtonian and/or the temperature breaks the laminar flow...– the reduction method becomes more accurate by increasing the number of base polynomial functions. At the same time it stays far more effective than a real 3D computation.*

5 Some examples of flows between two surfaces

The examples proposed here are compared with numerical results computed with the finite element software FIDAP (see **?**)). Its post-processor is also used to visualize the results obtained by the reduction method (which means the $(N-1)$D results are projected on a ND mesh).

5.1 Example 1: A convergent

This example is a simple test to check that the method gives correct results and to show the need of something more accurate than the Hele-Shaw approximation for quasi-cylindrical domains.

As it can be seen on the figures, the symmetry is satisfied: the x-velocity u_x only involves even polynomials ($u_{x1} = 0$ over ω). On the opposite u_y involves only odd polynomials (fig A1 and A2). The out-coming flux rate is twice as large as the income one as expected. To confirm this basic test we use a F.E.M. simulation on a very thin mesh which will be called the “exact” solution (fig. A4 and A6), and we compare it with our results.

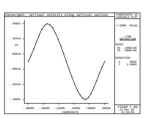

Fig. A1 u_y velocity

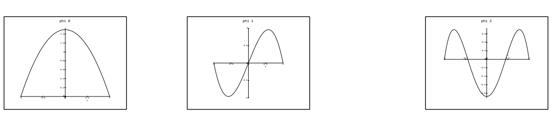

Fig. A2 : First three velocity polynoms φ_0, φ_1 and φ_2.

The results shown are computed with different numbers of polynomials (J=1, 2, 3 and 5), so that we can see their influence. In order, to see the differences between the results we have to look at the pressure field as the velocity fields are all the same with 3 or more functions (fig. A4).As expected, the results become more accurate when J increases, but the main observation is the good quality of the results with only 3 or 5 polynomials (fig. A9 and A10). They are better than the results obtained with the F.E.M. with 8 nodes over the thickness (fig. A5) which gives a larger matrix than our method with 5 polynomials.

The 1-polynomial results (fig. A3 and A7), which is the same than the Hele-Shaw one, satisfy the mass conservation but forget the vertical velocity and worst, gives bad pressure values.

On the figures, the x and y-scalings are the same.

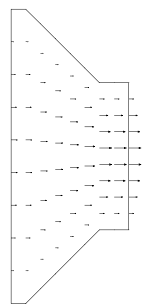

Fig. A3
1D+1, 1 fct

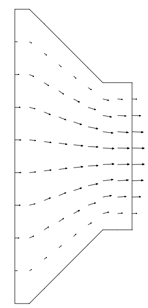

Fig. A4
correct velocities

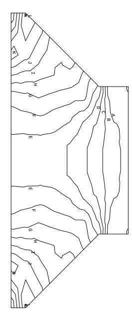

Fig. A5
2D with 8 nodes

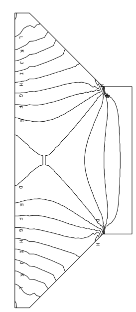

Fig. A6
2D, fine mesh

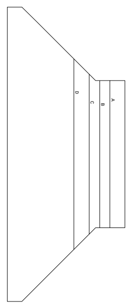

Fig. A7
1D+1, 1 fct

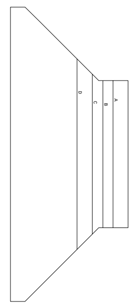

Fig. A8
1D+1, 2 fcts

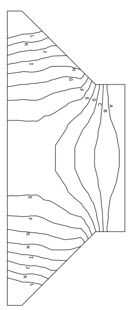

Fig. A9
1D+1, 3 fcts

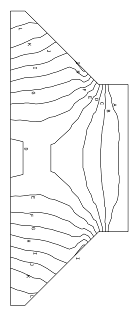

Fig. A10
1D+1, 5 fcts

5.2 *Example 2: Flow in a irregular shell*

In this case, the variations of the geometry in the thickness are quite smooth. However (Figs. 5-8) we can see differences in the results according to the method, in the quality and in the computation time needed.

Time computation are the one of the 3D example given in table 4. The method of reduction of the dimension is always much faster for a similar quality of result.

There is no reference model for this example since it would have needed a huge computation, however the evolution of the results with the increasing of the accuracy gives an idea of how should be the right solution.

The first case, with one polynomial function, gives almost the good result, but pressure is too hight on the last wave of the model and speed are locally too slow between the hole and the borders. With three functions, the pressure is correct and so seems to be the velocities. The F.E.M. results shows more instabilities, especially for the speed, but we recover the results of the reduction method.

6 Conclusion

The method described in this paper has proved its efficiency as far the thickness varies “smoothly”. It can capture the recirculations and depressions inside the thickness with just three polynomials and the computations have shown the rapid convergence of the approximated solution with J, the number of polynomials.

This method can be widely adapted to other kind of problems such flows including thermic , non-Newtonian flows... Transient equations, non linear ones (like the Navier-Stokes equations) can be dimensionally reduced too. Free surface problems can also be introduced, and for a mold injection problem, the formulation of the thickness would simplify the simulation of the frozen layer i.e. the simulation of free surfaces on the top, h^+, and bottom, h^-.

Other boundary conditions can be introduced with other kinds of polynomials. For example, an axi-symmetric simulation can be effected with a Neumann B.C. on h^+ and a Dirichlet B.C. on $h^- = 0$.

Last, the method needs much less polynomials than the F.E.M. needs nodes over the thickness for comparable results. This means a smaller associated linear problem for this method and consequently a faster computation.

Appendix A: Proofs of proposition 2.1, 2.4 and 2.6

Appendix A:.1 Proof of proposition 2.1

Proposition 2.1 *The Stokes problem with mixed boundary conditions (3) has a solution. This solution* $(\mathbf{u}, p) \in H^1(\Omega)^N \times L^2(\Omega)$ *is unique.*

Proof: First remove $\mathbf{g}$ in the Dirichlet boundary condition to get a homogeneous problem. This can be done since there exists $\mathbf{u_0} \in H^1(\Omega)^N$ such that

$$\left\{ \begin{array}{rcl} \nabla.\mathbf{u_0} & = & 0 \\ \mathbf{u_0}\Big|_{\Gamma_D} & = & \mathbf{g} \end{array} \right.$$

so that with $\mathbf{u} = \mathbf{u}^\star + \mathbf{u_0}$ one obtain a variational formulation of our problem: find $(\mathbf{u}^\star, p) \in H^1_{0,\Gamma_D}(\Omega)^N \times L^2(\Omega)$ such that $\forall \mathbf{v} \in H^1_{0,\Gamma_D}(\Omega)^N, \forall q \in L^2(\Omega)$

$$\left\{ \begin{array}{rcl} \nu < \nabla\mathbf{u}^\star, \nabla\mathbf{v} > - < p, \nabla.\mathbf{v} > & = & < \mathbf{l}, \mathbf{v} > \\ - < \nabla.\mathbf{u}^\star, q > & = & 0 \end{array} \right.$$

with $< \mathbf{l}, \mathbf{v} > = < \mathbf{f}, \mathbf{v} > + \nu < \nabla\mathbf{u_0}, \nabla\mathbf{v} > - < -\nu\dfrac{\partial\mathbf{u_0}}{\partial n}, \mathbf{v} >_{\Gamma_N}$ and $H^1_{0,\Gamma_D}(\Omega) = \{v \in H^1(\Omega), v|_{\Gamma_D} = 0\}$.

Using the usual notation $a(\mathbf{u}, \mathbf{v}) = < \nabla\mathbf{u}, \nabla\mathbf{v} >$ and $b(\mathbf{v}, q) = - < q, \nabla.\mathbf{v} >$, the above system can be written as:

$$\left\{ \begin{array}{rcll} \nu\, a(\mathbf{u}^\star, \mathbf{v}) + b(\mathbf{v}, p) & = & < \mathbf{l}, \mathbf{v} >_{V' \times V} & \forall \mathbf{v} \in V \\ b(\mathbf{u}^\star, p) & = & 0 & \forall q \in Q \end{array} \right.$$

where $V = H^1_{0,\Gamma_D}(\Omega)^N$ and $Q = L^2(\Omega)$ are respectively equipped with the norms:

$$\begin{array}{rcl} ||\mathbf{v}||_V & = & \left(\displaystyle\int_\Omega |\nabla\mathbf{v}|^2 + \mathbf{v}^2 \, dx_\omega \right)^{1/2} \\ ||q||_Q & = & \left(\displaystyle\int_\Omega q^2 \, dx_\omega \right)^{1/2} \end{array}$$

This system has a unique solution if the Inf-Sup condition (see **?**)) is satisfied, i.e., if

$$\inf_{q \in Q} \sup_{\mathbf{v} \in V} \frac{b(\mathbf{v}, q)}{||\mathbf{v}||_V ||q||_Q} \geq \beta > 0.$$

In order to verify this condition we first build for any $q \in Q$ a function $\mathbf{v} \in V$ such that $\nabla.\mathbf{v} = -q$. Introduce a function $\mathbf{e} = c\rho\mathbf{n}$ on Γ_N and 0 on Γ_D with ρ defined as

$$\rho(x_N) = \left\{ \begin{array}{lll} e^{\frac{-1}{1-4y^2}} & \text{if} & |y| < 1/2, \\ 0 & \text{if } 1/2 < & |y| < 1, \end{array} \right.$$

and the constant c chosen such that

$$\int_{\partial\Omega} \mathbf{e}.\mathbf{n} \, ds = -\int_\Omega q \, ds,$$

i.e.,

$$c = -\frac{\int_\Omega q \, ds}{\int_{\Gamma_N} \rho \, dx_N}.$$

Therefore:

$$\begin{array}{rcl} ||\mathbf{e}||_{H^{1/2}(\partial\Omega)} & = & |c| \; ||\rho||_{H^{1/2}(\Gamma_N)} \\ & \leq & \dfrac{meas(\Omega)^{1/2} \, ||q||_{0,\Omega}}{|\int_{\Gamma_N} \rho \, ds|} \; ||\rho||_{H^{1/2}(\Gamma_N)} \\ & \leq & C_1 \, ||q||_{0,\Omega} \end{array}$$

Consider now the function $\mathbf{w} \in H^1(\Omega)^N$ solution of

$$\left\{ \begin{array}{rcl} -\Delta\mathbf{w} + \mathbf{w} & = & 0, \\ \mathbf{w}|_{\partial\Omega} & = & \mathbf{e}. \end{array} \right.$$

Obviously $||\mathbf{w}||_1 = ||\mathbf{e}||_{H^{1/2}(\partial\Omega)}$ since $||\mathbf{w}_{|\Gamma}||_{1/2} := \inf_{\substack{\mathbf{v}_{|\Gamma} = \mathbf{e} \\ \mathbf{v} \in H^1}} ||\mathbf{v}||_{1,\Omega}$.

The divergence operator $\nabla.$ is an isomorphism from $\{\mathbf{v} \in H^1_0(\Omega)^N; \nabla.\mathbf{v} = 0\}^\perp$ onto $L^2_0(\Omega) = \left\{ p \in L^2(\Omega); \int_\Omega p \, dx_\omega = 0 \right\}$ (see **?**)). Therefore, since $-q - \nabla.\mathbf{w} \in L^2_0(\Omega)$, there exists $\mathbf{z} \in H^1_0(\Omega)^N$ such that $\nabla.\mathbf{z} = q - \nabla.\mathbf{w}$. Consequently:

$$|\mathbf{z}|_{1,\Omega} \leq C_2 \left(||q||_0 + ||\mathbf{w}||_1 \right) \leq C_3 \, ||q||_{0,\Omega}.$$

Finally, let $\mathbf{v} = \mathbf{z} + \mathbf{w}$, so that $\nabla.\mathbf{v} = -q$, $\mathbf{v} \in V$ and

$$|\mathbf{v}|_{1,\Omega} \leq C_4 ||q||_{0,\Omega}.$$

Since the H^1 semi-norm is equivalent to the H^1 norm on V, we have

$$||\mathbf{v}||_{1,\Omega} \leq C_5 ||q||_{0,\Omega}$$

and the Inf-Sup condition holds since

$$\forall q \in Q \;\; \exists \mathbf{v} \in V \;\; \text{s.t.} \;\; \frac{b(\mathbf{v}, q)}{||\mathbf{v}||_1 \, ||q||_0} = \frac{||q||_0}{||\mathbf{v}||_1} \geq \frac{1}{C_5} > 0$$

The bilinear functional $a(u, v) = < \nabla\mathbf{u}, \nabla\mathbf{v} >$ is H^1_{0,Γ_N} elliptic and the Inf-Sup condition is satisfied hence our problem has a unique solution in $H^1_{0,\Gamma_N}(\Omega)^N \times L^2(\Omega)$, (see **?**)). $\diamond$

Appendix A:.2 Proof of proposition 2.4

For any function $\mathbf{v} \in \hat{V}$ one can find a sequence $\mathbf{v}^J$ that converges to $\mathbf{v}$ in $\hat{V}$.

Since $\bigcup_{J=0}^{\infty} \mathbf{P}_J(-1,1)$ is dense in $L^2(-1,1)$ and since the $(J+1)$ first Legendre polynomials form a basis of $\mathbf{P}_J(-1,1)$

$$\forall f \in L^2(\omega, L^2(-1,1)),\ f(x_\omega, x_N) = \textstyle\sum_{j=0}^{\infty} f_j(x_\omega)\psi_j(x_N) \quad \text{a.e. in } x_\omega.$$

This series converges in $L^2(\hat{\Omega})$ by applying the dominated convergence theorem.

The same proof and proposition 2.3, show that:

$$\forall f \in L^2(\omega, L^2_w(-1,1)),\ f(x_\omega, x_N) = \textstyle\sum_{j=0}^{\infty} f_j(x_\omega)\varphi_j(x_N) \quad \text{a.e. in } x_\omega$$

where $f_j \in L^2(\omega)$ and this series converges in $L^2(\omega, L^2_w(-1,1))$.

Since $\hat{V} = L^2(\omega, H^1_0(-1,1))^N \cap H^1_0(\omega, L^2(-1,1))^N$, and because H^1_0 is a subset of L^2_w, we have:

$$\forall \mathbf{v} \in \hat{V}, \quad \mathbf{v}(x_\omega, x_N) = \sum_{j=0}^{\infty} \mathbf{v}_j(x_\omega)\varphi_j(x_N) \quad \text{a.e. in } x_\omega$$

and this series converges in $L^2(\omega, L^2_w(-1,1))^N$ hence in $L^2(\hat{\Omega})^N$.

Let $\mathbf{v}^J = \displaystyle\sum_{j=0}^{J} \mathbf{v}_j(x_\omega)\,\varphi_j(x_N)$.

Since $\mathbf{v}_j = \dfrac{1}{||\varphi_j||}\displaystyle\int_{-1}^{1} \mathbf{v}\varphi_j\, dx_N$, $\mathbf{v}_j \in H^1(\omega)^N$.

On the other hand, assume $\mathbf{v} \in H^2(\hat{\Omega})^N \cap H^1_0(\hat{\Omega})^N$, then $\dfrac{\partial \mathbf{v}}{\partial x_\omega}(x_\omega, x_N) \in L^2(\omega, L^2_w(-1,1))$ and one can write $\frac{\partial \mathbf{v}}{\partial x_\omega}(x_\omega, x_N) = \sum_{j=0}^{\infty} \tilde{\mathbf{v}}_j(x_\omega)\,\varphi_j(x_N)$.

One can check that $\displaystyle\int_0^x \tilde{\mathbf{v}}_j\, dt = \mathbf{v}_j$ with $\omega = [0,1]$ and the homogeneous Dirichlet boundary condition in $x = 0$ i.e. $\tilde{\mathbf{v}}_j = \dfrac{\partial \mathbf{v}_j}{\partial x_\omega}$.

Applying the same proof and knowing that $\varphi'_j = -(2j+3)\psi_{j+1}$, one has:

$$\frac{\partial \mathbf{v}^J}{\partial x_N}(x_\omega, x_N) = \sum_{j=0}^{J} \mathbf{v}_j(x_\omega)\,\varphi'_j(x_N) \text{ converges in } L^2 \rightarrow \frac{\partial \mathbf{v}}{\partial x_N}.$$

Hence, if $\mathbf{v} \in H^2 \cap H^1_0$, there exists a sequence $\mathbf{v}^J \in V_J$ such that $\mathbf{v}^J \rightarrow \mathbf{v}$ in H^1. Since $H^2 \cap H^1_0$ is dense in H^1_0, the general result follows by the diagonal argument. ◇

Appendix A:.3 Proof of proposition 2.6

Define $\Pi^{1,0}_J$ the operator of L^2_w-projection from $\hat{V}$ into V_J:

$$\Pi^{1,0}_J \mathbf{v}(\hat{x}_\omega, \hat{x}_N) = \sum_{j=0}^{J} \mathbf{v}_j(\hat{x}_\omega)\,\varphi_j(\hat{x}_N). \tag{45}$$

This operator defines also a H_{1y}-projection (i.e. for the H_1-semi-norm in x_N):

$$\begin{aligned}
&\int_{-1}^{1} \frac{\partial(\mathbf{v} - \Pi^{1,0}_J \mathbf{v})}{\partial x_N}(\hat{x}_\omega, \hat{x}_N)\varphi'_k(\hat{x}_N)\, d\hat{x}_N \\
&\quad = \int_{-1}^{1} \sum_{j=J+1}^{\infty} \mathbf{v}_j(\hat{x}_\omega)\,(-(2j+3)\psi_{j+1}(\hat{x}_N)) \\
&\qquad (-(2k+3)\psi_{k+1}(\hat{x}_N))\, d\hat{x}_N \\
&\quad = 0 \qquad \forall k = 0..J
\end{aligned}$$

since $k < j$ and the ψ_j are the Legendre polynomials.

To prove the proposition, the Inf-Sup condition (see **?**)) has to be satisfied for the discrete problem. Since the continuous Inf-Sup condition is already satisfied, it will carry to the reduced problem if one can show that (see **?**)):

$$\hat{b}(\Pi^{1,0}_J \mathbf{v} - \mathbf{v}, q^J) = 0 \quad \forall q^J \in Q_J \quad \forall \mathbf{v} \in \hat{V} \tag{46}$$

$$||\Pi^{1,0}_J \mathbf{v}||_{V_J} \leq C\,||\mathbf{v}||_{\hat{V}} \tag{47}$$

Since $\Pi^{1,0}_J$ is an orthogonal projection with respect to the inner product of L^2_w and to the product of the H_1-semi-norm in x_N, inequality (47) is satisfied.

To check (46) first split $\hat{b}$:

$$\hat{b}(\Pi^{1,0}_J \mathbf{v} - \mathbf{v}, q^J) = -\textstyle\int_{\hat{\Omega}} \tilde{\nabla}.(\Pi^{1,0}_J \mathbf{v} - \mathbf{v})q^J\, ds = X_1 + X_2 \quad \forall q^J \in Q_J$$

where

$$\begin{aligned}
X_1 &= -\int_{\hat{\Omega}} \left(\frac{\partial}{\partial \hat{x}_\omega} + \frac{\partial \hat{x}_N}{\partial x_o m}\frac{\partial}{\partial \hat{x}_N}\right)(\Pi^{1,0}_J v_1 - v_1)(\hat{x}_\omega, \hat{x}_N) \\
&\qquad \sum_{j=0}^{J} q_j(\hat{x}_\omega)\psi_j(\hat{x}_N)\, d\hat{x}_\omega\, d\hat{x}_N \\
X_2 &= -\int_{\hat{\Omega}} \frac{\partial \hat{x}_N}{\partial x_N}\frac{\partial}{\partial \hat{x}_N}(\Pi^{1,0}_J v_2 - v_2)(\hat{x}_\omega, \hat{x}_N) \\
&\qquad \sum_{j=0}^{J} q_j(\hat{x}_\omega)\psi_j(\hat{x}_N)\, d\hat{x}_\omega\, d\hat{x}_N
\end{aligned}$$

Here again one assume $\mathbf{v} \in H^2$ to get the convergence in L^2 of the series $\sum \frac{\partial v_{1j}}{\partial \hat{x}_\omega}$ and conclude by density. Therefore since

$$\frac{\partial}{\partial \hat{x}_\omega}(\Pi_J^{1,0} v_1 - v_1) = -\sum_{j=J+1}^{\infty} \frac{\partial v_{1j}}{\partial \hat{x}_\omega}(\hat{x}_\omega)\varphi_j(\hat{x}_N)$$

$$= -\sum_{j=J+1}^{\infty} F_j(\hat{x}_\omega)\psi_j(\hat{x}_N)$$

$$\text{with} \qquad F_j(\hat{x}_\omega) = (\frac{\partial v_{1j}}{\partial \hat{x}_\omega} - \frac{\partial v_{1(j-2)}}{\partial \hat{x}_\omega})(\hat{x}_\omega),$$

the first part of X_1 is

$$X_{11} = -\int_{\hat{\Omega}} \sum_{j=J+1}^{\infty} F_j(\hat{x}_\omega)\psi_j(\hat{x}_N) \sum_{j=0}^{J} q_j(\hat{x}_\omega)\psi_j(\hat{x}_N)\, d\hat{x}_\omega\, d\hat{x}_N.$$

The first series belongs to the L^2-orthogonal complement of the space spanned by the $J+1$ first Legendre polynomials($\mathbf{L}_J$) and the second series belongs to $\mathbf{L}_J$, therefore $X_{11} = 0$.

In the second part of X_1, expand the partial derivative (cf formulae (12)):

$$\begin{aligned} X_{12} = & -\int_{\hat{\Omega}} (H(\hat{x}_\omega) + G(\hat{x}_\omega)\hat{x}_N)\frac{\partial}{\partial \hat{x}_N}(\Pi_J^{1,0} v_1 - v_1)(\hat{x}_\omega, \hat{x}_N) \\ & \sum_{j=0}^{J} q_j(\hat{x}_\omega)\psi_j(\hat{x}_N)\, d\hat{x}_\omega\, d\hat{x}_N \\ = & -\int_{\hat{\Omega}} H(\hat{x}_\omega)\frac{\partial}{\partial \hat{x}_N}(\Pi_J^{1,0} v_1 - v_1)(\hat{x}_\omega, \hat{x}_N) \\ & \sum_{j=0}^{J} q_j(\hat{x}_\omega)\psi_j(\hat{x}_N)\, d\hat{x}_\omega\, d\hat{x}_N \\ & -\int_{\hat{\Omega}} G(\hat{x}_\omega)\frac{\partial}{\partial \hat{x}_N}(\Pi_J^{1,0} v_1 - v_1)(\hat{x}_\omega, \hat{x}_N) \\ & \sum_{j=0}^{J+1} \tilde{q}_j(\hat{x}_\omega)\psi_j(\hat{x}_N)\, d\hat{x}_\omega\, d\hat{x}_N \end{aligned}$$

An integration by parts in $\hat{x}_N$ gives

$$\begin{aligned} X_{12} = & \int_\omega \int_{-1}^{1} H(\hat{x}_\omega) \sum_{j=J+1}^{\infty} v_{2j}(\hat{x}_\omega)\,\varphi_j(\hat{x}_N) \\ & \sum_{j=0}^{J} q_j(\hat{x}_\omega)\,\psi'_j(\hat{x}_N)\, d\hat{x}_N\, d\hat{x}_\omega \\ & + \int_\omega \int_{-1}^{1} G(\hat{x}_\omega) \sum_{j=J+1}^{\infty} v_{2j}(\hat{x}_\omega)\,\varphi_j(\hat{x}_N) \\ & \sum_{j=0}^{J} \overline{q}_j(\hat{x}_\omega)\,\psi_j(\hat{x}_N)\, d\hat{x}_N\, d\hat{x}_\omega. \end{aligned}$$

Once again the first series belongs to the L^2-orthogonal complement of $\mathbf{L}_J$ and the second series belongs to $\mathbf{L}_J$, therefore $X_{12} = 0$.

The same proof gives $X_2 = 0$.

Hence (46) is satisfied for all $q \in Q_J$ and so is the discrete Inf-Sup condition applied to our reduced problem:

$$\sup_{\mathbf{v}\in V^J} \frac{\hat{b}(\mathbf{v}, q)}{\|\mathbf{v}\|_{V^J}} \geq \beta \|q\|_{Q^J} \qquad \forall q \in Q^J \tag{48}$$

Therefore problem (17) has a unique solution $(\mathbf{u}^J, q^J)$ in $V_J \times Q_J$. $\diamond$

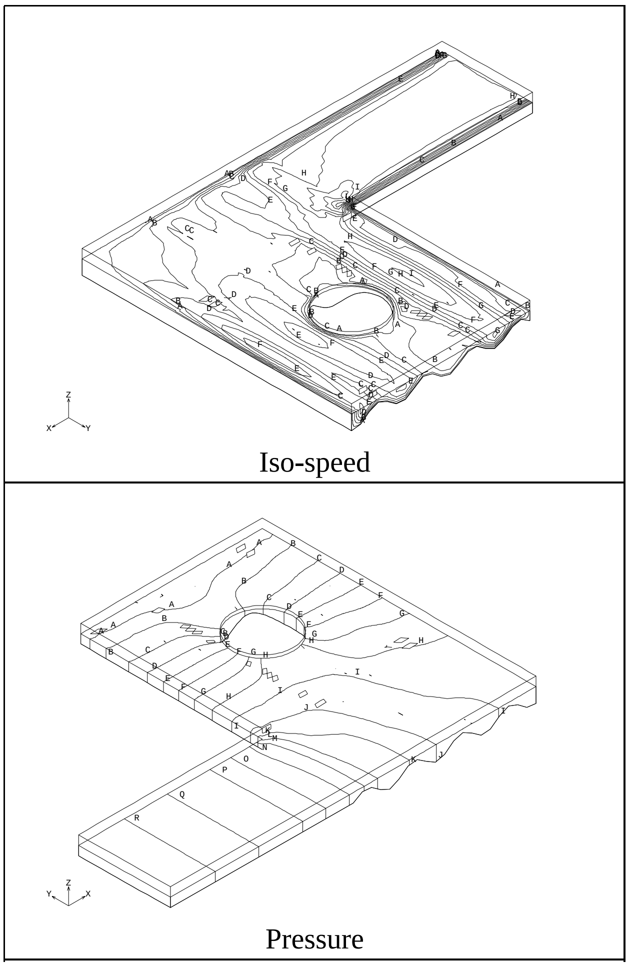

Figure 5 : with the reduction method and 3 functions in the thickness

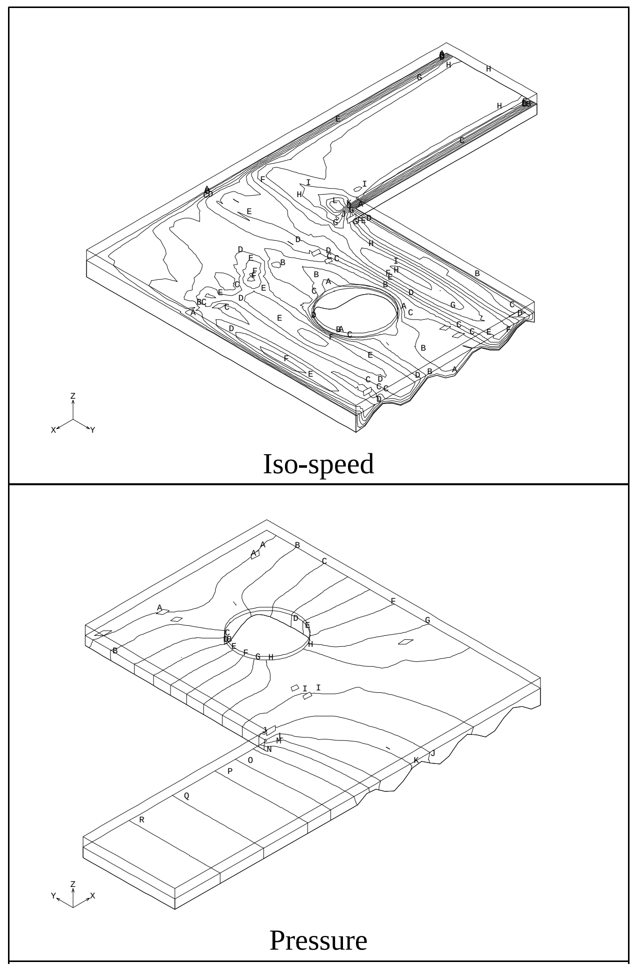

Figure 6 : with the F.E.M. and 5 nodes in the thickness

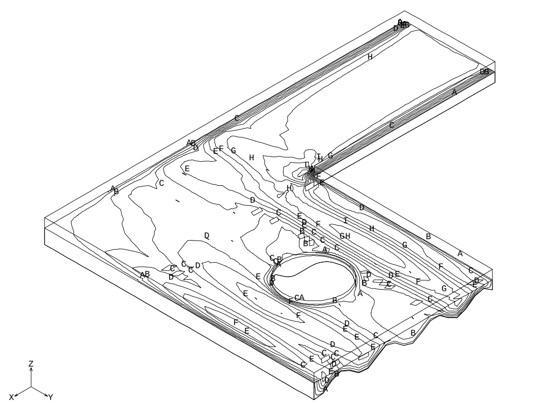

Iso-speed

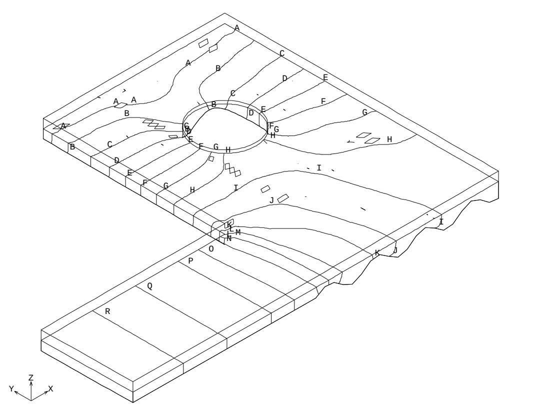

Pressure

Figure 7 : with the reduction method and 5 functions in the thickness

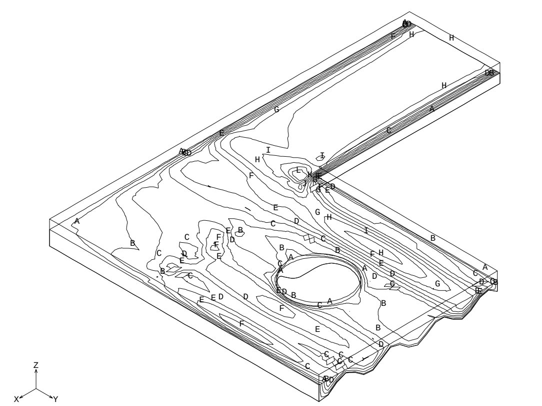

Iso-speed

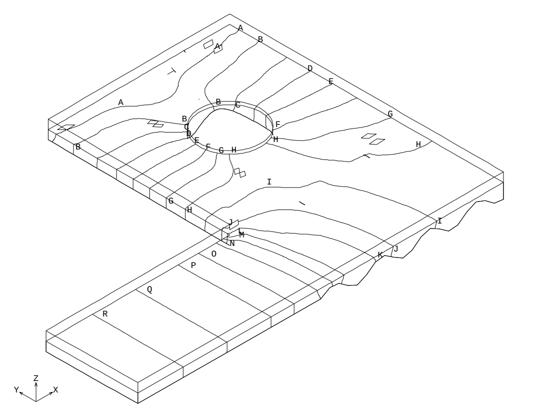

Pressure

Figure 8 : with the F.E.M. and 9 nodes in the thickness